Local Mode Analysis of
2D ICRF Wave Solutions

D.A. D'Ippolito,[1] J.R. Myra,[1] E.F. Jaeger,[2] L.A. Berry,[2] D.B. Batchelor[2]

[1]*Lodestar Research Corporation, Boulder, Colorado;* [2]*ORNL, OakRidge, Tennessee*

Abstract. Numerical techniques (windowed Fourier transforms and wavelets) are developed for carrying out a local mode analysis $\mathbf{k}(\mathbf{x})$ of ICRF field solutions. It is shown that simultaneous resolution of long- and short-wavelength waves in typical rf mode conversion scenarios requires the use of a modified wavelet transform. The ability to get quantitative information by this technique is assessed and visualization techniques for wave polarization information are illustrated.

INTRODUCTION

With the growing capability of rf simulations,[1-3] there is a strong motivation to develop appropriate post-processing tools for extracting physical information from the numerical solutions. Full-wave ICRF codes yield complicated rf field patterns, and the challenge is to understand these patterns by appealing to the intuitive, but approximate, physics-based notion of local plasma modes (global eigenmodes, transmitted and reflected waves, and mode conversions between different types of waves). Quantitative information on the local wavevectors, amplitudes and wave polarizations is required for a basic understanding of the plasma heating and the ICRF-driven currents and flows. As part of the rf SciDAC project, numerical techniques (windowed Fourier transforms and wavelets) have been investigated for the local mode analysis of ICRF field solutions. Here, we illustrate these techniques for a DIII-D D(H) mode conversion reference case[4] computed by the AORSA-1D code, which includes a model of the 2D poloidal magnetic field. Work is in progress to apply the techniques described in this paper to full 2D rf wave solutions.

TRANSFORM METHODS

We illustrate these methods by considering the 1D case where the function f(x) is represented by its values $f_i = f(x_i)$ on a grid of N spatial points x_i. The transform specifies the mapping $f(x) \rightarrow F(k)$ where $k = k_x$ is also represented on a grid of N points. Here, we analyze $\mathbf{E}(x)$ obtained from a fast wave (FW) to ion Bernstein wave (IBW) or ion cyclotron wave (ICW) mode-conversion solution with $x = R - R_0$ and $\mathbf{k} = k_x \mathbf{e}_x + (n/R) \mathbf{e}_z$, where R is the major radius of the tokamak and n is the toroidal mode number. Our tests of various transform methods are described below.

The simplest approach is to use the *discrete Fourier transform* to resolve the wave propagation data into global k modes. This identifies all the relevant physical modes in the spatial domain of interest but does not yield any information as to their spatial location, nor does it yield insight into relationships among modes such as mode conversion. To resolve this difficulty, we considered the *Windowed Fourier Transform* (WFT) technique, in which the function $E(x)$ is multiplied by a window $w(x)$ before carrying out the transform. The best results are obtained using a smooth window function such as the Gaussian $w(x) = Exp[-(x-x_0)^2/(2x_w^2)]$, where x_0 and x_w are the location and width of the window. The WFT method *with a constant window width* works well for a single wave or for the case of multiple waves with similar wavelengths, but it fails for the case of multiple waves with very different wavelengths, such as occurs in mode conversion. For example, a large window is needed to resolve the wavelength (or k) of the FW but does a poor job in giving the spatial location of the IBW; a small window does a good job in localizing the IBW in space but does a poor job in resolving the FW wavelength.

An analysis of this problem shows that it stems from the need to minimize two conflicting types of errors: (1) the "Heisenberg" error $\Delta k_1 = C\pi/\Delta x$, where C is a constant of order unity and Δx is the size of the region in which the transform is carried out (here, the window width), and (2) the "non-local" or "gradient" error $\Delta k_2 \approx (\partial k/\partial x)\,\Delta x$, where $k(x)$ is the local (eikonal) wavenumber. Note that Δk_1 vanishes in for a large window, whereas Δk_2 is reduced by a small window. The competition between the two effects produces an "optimal" window width which depends on the wavelength, i.e. $x_w = x_w(k)$. Thus, we must generalize the WFT technique to have a window width that scales with k.

A transform involving basis functions that are translated and scaled is called a "wavelet." The *Morlet wavelet* is essentially a WFT with a scaled Gaussian window, $x_w = c_0/k$, where c_0 is a constant that has an optimal value ($c_0 = 5$) for minimizing the error. This wavelet is an improvement over the WFT, but the scaling breaks down at $k = 0$. The infinite window width at $k = 0$ leads to large gradient error and false peaks in the spectrum. However, it is essential in treating the FW to IBW mode conversion problem that one resolve k's of both signs and therefore handle the behavior at $k = 0$.

We have developed a simple modification to the Morlet wavelet that keeps its useful features while still resolving the $k = 0$ region. We scale the window width as $x_w = c_0/(k^2 + k_0^2)^{1/2}$ so that $x_w \to c_0/k_0$ as $k \to 0$, where k_0 is a constant. While $k_0 \neq 0$ spoils the pure wavelet scaling in a small region, it permits us to obtain a physical answer over the whole x-k plane. We call this approach the "*k-wavelet*" method. It should be emphasized that we do not need the "pure" wavelet scaling for our application. We are simply using the wavelet transform for visualization and for extracting the dispersion function $k(x)$. We will show that the k-wavelet method provides a useful tool for graphically obtaining this information.

The k-wavelet transform is implemented in *Mathematica* using fast Fourier transform (FFT) techniques as follows. The wavelet transform $f(x) \to W(x_0, k)$ involves a spatial convolution of the functions $f(x)$ and a mother wavelet $\Psi(x)$. Using the convolution theorem to cast this into k-space reduces the number of computations from N^2 to $N \ln N$. Thus, we define the k-wavelet transform $W(x_0, k)$ as

$$W(x_0, k) = \frac{1}{N} \Im^{-1} \left(\Im[f(x)] \, \Im[\Psi*(k, x - x_0)] \right) , \qquad (1)$$

where $\Im[f(x)]$ denotes the forward FFT of $f(x)$, $\Im^{-1}$ denotes the inverse FFT, and Ψ is the k-wavelet function defined by

$$\Psi[k, \, x - x_0] = \exp[i \, k(x - x_0)] \exp\left[-(x - x_0)^2 / (2 \, x_w{}^2) \right] , \qquad (2)$$

with $x_w(k) = c_0/(k^2 + k_0{}^2)^{1/2}$ and c_0, k_0 are constants. In the limit $k_0 \to 0$, $\Psi \to \Psi[k(x - x_0)]$ and the exact wavelet scaling is recovered.

APPLICATIONS AND CONCLUSIONS

We first consider a DIII-D D(H) mode conversion reference case[4] computed by the AORSA-1D code, which includes a model of the 2D poloidal magnetic field B_p. We define the k-wavelet spectral power density $P_\alpha(x_0, k) = |W_\alpha(x_0, k)|^2$, where W_α is the k-wavelet transform of $E_\alpha(x)$ defined in Eq. (1). In Fig. 1 we show the contours of $P_\perp(x0, k) = P_x(x_0, k) + P_y(x_0, k)$, obtained by analyzing the AORSA-1D code solutions for two values of B_p corresponding to horizontal slices of the 2D equilibrium. The wavelet analysis illustrates the important result[5,2] that the mode conversion process is sensitive to the poloidal magnetic field. Above the midplane [Fig. 1(a)] the incoming FW converts to a backward-propagating IBW, whereas below the midplane [Fig. 1(b)] the FW converts to a forward-propagating ICW.
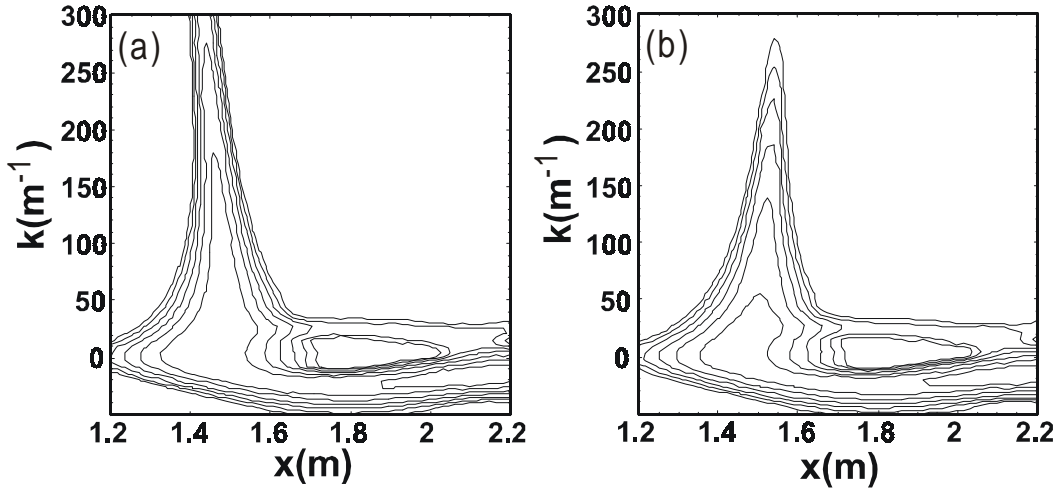
FIGURE 1. k-wavelet transform spectral power density $P_\perp(x_0, k)$ of the rf electric field with $c_0 = 5$ and $k_0 = 40$ m^{-1} for horizontal slices (a) above the midplane, and (b) below the midplane.

A comparison of the contours in Fig. 1(a) with the analytic 1D hot-plasma dispersion relation for the same parameters shows good agreement for the k contours of the incident and reflected FW and the IBW and for the location of the mode conversion surface (near $x = 1.5$ m). Thus, the k-wavelet transform is useful for obtaining quantitative information about the spatial dependence of the wavenumber.

We have also investigated the use of the wavelet analysis for simultaneous visualization of dispersion, amplitude and wave polarization information in 3D plots by the use of appropriately defined color palettes. In Fig. 2, we show a grayscale print of a 3D plot for the case of Fig. 1(a) with palette chosen to reflect the linear wave polarization, E_x/E_y. A color version of this figure can be viewed in the version of this paper posted on our website.[6]
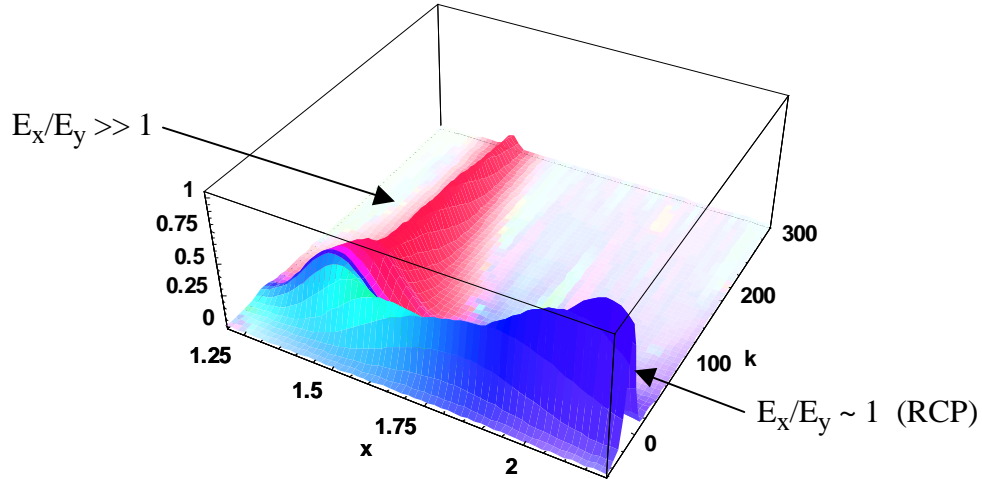
FIGURE 2. k-wavelet transform of $P_\perp(x_0, k)$ of the rf electric field using the same parameters as Fig. 1(a); the color palette indicates the *linear* wave polarization E_x/E_y.

We have shown that the "k-wavelet" transform provides a useful diagnostic for wave properties in complex situations such as mode conversion where multiple waves with vastly different wavelengths are present simultaneously. The methods used here can be generalized to obtain the wavevector $\mathbf{k}_\perp = (k_x, k_y)$ for 2D rf field solutions, $\mathbf{E} = \mathbf{E}(x,y)$. However, the 1D analysis illustrated here is qualitatively valid when $k_y \ll k_x$, which is satisfied for the case shown here.

ACKNOWLEDGMENTS

REFERENCES

1. E.F. Jaeger, L.A. Berry, E. D'Azevedo, D. B. Batchelor *et al.*, Phys. Plasmas **9**, 1873 (2002).
2. E.F. Jaeger, L.A. Berry, J. R. Myra, D. B. Batchelor *et al.*, Phys. Rev. Lett. **90**, 195001 (2003).
3. P.T. Bonoli, J.C. Wright, Y. Lin, M. Porkolab *et al.*, Bull. APS **47**, 141 (2002), paper GO1 13.
4. E.F. Jaeger, L. A. Berry, E. D'Azevedo *et al.*, Phys. Plasmas **8**, 1573 (2001).
5. E. Nelson-Melby, M. Porkolab, P. T. Bonoli, *et al.*, Phys. Rev. Lett. **90**, 155004 (2003).
6. D.A. D'Ippolito, J.R. Myra *et al.*, http://www.lodestar.com/LRCreports/kwavelets.pdf .